Hindawi Publishing Corporation
Journal of Nanomaterials
Volume 2016, Article ID 3040536, 5 pages
http://dx.doi.org/10.1155/2016/3040536

Research Article

Effect of Na Doping on the Nanostructures and Electrical Properties of ZnO Nanorod Arrays

Lu Yue,[1,2] Zhiqiang Zhang,[1,2] Yanyan Ma,[1,2] and Wenhui Zhang[1,2]

[1]*Jiangsu Collaborative Innovation Center for Ecological Building Materials and Environmental Protection Equipment, Yancheng Institute of Technology, Yancheng 224051, China*
[2]*Key Laboratory for Advanced Technology in Environmental Protection of Jiangsu Province, Yancheng Institute of Technology, Yancheng 224051, China*

Correspondence should be addressed to Wenhui Zhang; zwhuizi000@sina.com

Received 9 March 2016; Accepted 5 May 2016

Academic Editor: Gongming Wang

The p-type ZnO nanorod arrays were prepared by doping Na with hydrothermal method. The structural, electrical, and optical properties were explored by XRD, Hall-effect, PL, and Raman spectra. The carrier concentrations and the mobility of Na-doped ZnO nanorod arrays are arranged from 1.4×10^{16} cm^{-3} to 1.7×10^{17} cm^{-3} and 0.45 cm^2 v^{-1} s^{-1} to 106 cm^2 v^{-1} s^{-1}, respectively.

1. Introduction

Zinc oxide (ZnO) is a promising material candidate for photoelectronic devices due to its direct wide electron energy bandgap of 3.37 eV at room temperature and large exciton binding energy of 60 meV. ZnO is conventionally used as a substrate for GaN and has advantages over GaN such as larger exciton binding energy, lower refraction index, and shallower acceptor levels. Despite its advantages over GaN, the application of ZnO in optoelectronics is hampered by the lack of stable p-type doping due to self-compensation by donor-like native defects, low solubility of p-type dopants, and formation of deep acceptor levels [1]. The n-type ZnO is available even without any intentional doping, but it is very difficult to dope ZnO p-type. Many groups have realized p-type ZnO conversion by doping group V elements (N [2], P [3], As [4], and Sb [5]) and groups I and IB (Li [6], Na [7–9], K [10], Ag [11], and Cu [12]), but the stability was not good. Among the group V elements, N is the most suitable dopant because it has about the same ionic radius as O and thus should readily be substituted on O sites. Indeed, it remains difficult to achieve good quality p-type conduction in N-doped ZnO due to either a low dopant solubility or a high defect ionization energy. Theoretically, group I element substituted on Zn sites is shallow acceptors [13], but instead these dopants tend to occupy the interstitial sites, partly due to their small atomic radius, and therefore act mainly as donors. On the other hand, reports of Na-doped p-type ZnO films are rather poor [14]. Up to now, various methods have been employed to prepare p-type ZnO including molecular beam epitaxy (MBE) [15], chemical vapor deposition [16], and pulsed laser deposition [17], in which complicated, high temperature deposition and expensive vacuum systems have been employed. In contrast, the hydrothermal method was proven to be an ideal technique for the development of p-type ZnO films owing to its simplicity and easy control of the composition at low cost [18–20]. To date, there is no report of Na doping of p-type ZnO nanorods by a hydrothermal method. Here, we report a simple, reliable, and low-cost method for growing and doping p-type ZnO nanorod arrays in aqueous solution, with Na as the p-type dopant.

2. Experimental Section

A high-resistance Si (100) wafer, the resistivity of which is above 500 Ω cm, was used as the substrate. Precleaned silicon substrate was coated with a ZnO seed layer by sol-gel spin coating. $Zn(AC)_2 \cdot 2H_2O$ were first dissolved in the mixture of 2-methoxyethanol and monoethanolamine. The molar ratio of monoethanolamine to $Zn(AC)_2 \cdot 2H_2O$ was maintained at 1 : 1 and the concentration of $Zn(AC)_2 \cdot 2H_2O$ was 75 mM. The sol was aged for 24 h at room temperature. The above

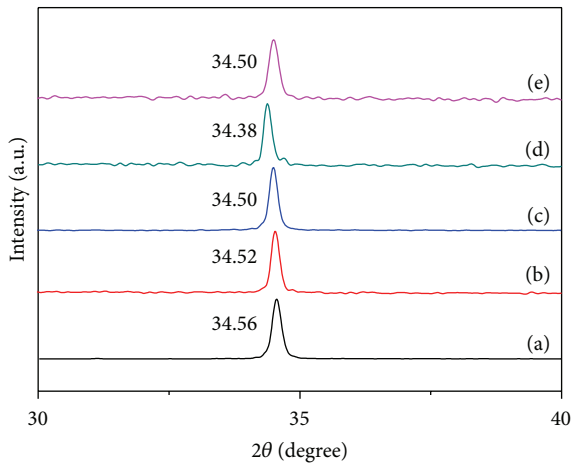

Figure 1: XRD patterns of the samples with n_{Na}/n_{Zn} of (a) 0, (b) 2.8, (c) 5.6, (d) 8.4, and (e) 11.2.

solution was then spin-coated at 500 rpm for 15 s and then at 5000 rpm for 60 s, followed by drying at 120°C for 15 min. The procedure from coating to drying was repeated five times before the substrates were placed into a 360°C tube furnace in air for 20 min to form ZnO seed layer, evaporate the solvent, and remove any organic residue. Subsequently, ZnO nanorod arrays were grown directly by placing the substrate at the bottom of the beaker in 20 mL of aqueous solution of 12.5 mM $Zn(AC)_2{\cdot}2H_2O$, 12.5 mM hexamethylenetetramine (HMTA, $C_6H_{12}N_4$), and different amounts of NaCl in a 50 mL autoclave. Different Na doping levels were obtained by varying the molar ratio of Na/Zn (n_{Na}/n_{Zn}) (0, 2.8, 5.6, 8.4, and 11.2) in the precursor solution. Finally the autoclave was sealed and heated at 95°C for 2 h. Subsequently, the samples are washed with deionized water for several times to remove the residual salt and amino complex and dried in a flow of nitrogen gas.

Powder X-ray diffraction (XRD) analyses were performed on a Philips PW-1830 X-ray diffractometer with Cu Kα irradiation (λ = 1.5406 Å) at a scanning speed of 0.014°/sec over the 2θ range of 30–40°. The electronic morphology of the samples was examined by Hitachi S-4800 scanning electron microscope (SEM). The electrical properties were characterized by a Hall effect measurement system. Photoluminescence and Raman spectra of samples on Si substrate were recorded using Jobin-Yvon Lab-Ram high-resolution spectrometer with He-Cd laser (λ = 325 nm).

3. Results and Discussion

XRD patterns of the hydrothermally grown samples were shown in Figure 1. The strong peak corresponding to ZnO (002) is observed in each film, which indicates high c-axis oriented in all samples. It can be seen that the diffraction peak shows an obvious shift to a smaller angle of about 34.56, 34.52, 34.50, 34.38, and 34.52 for the sample with n_{Na}/n_{Zn} of 0, 2.8, 5.6, 8.4, and 11.2, respectively. This demonstrates that Na doping increases the lattice constant as a result of larger ionic radius of Na^+ (0.089 nm) compared with that of Zn^{2+} (0.070 nm) [8].

Table 1: Electrical properties of ZnO films at room temperature.

n_{Na}/n_{Zn}	Carrier type	Mobility ($cm^2\ v^{-1}\ s^{-1}$)	Carrier concentration (cm^{-3})
0	n	40	1.4×10^{16}
2.8	p	106	3.1×10^{16}
5.6	p	41.9	1.7×10^{17}
8.4	p	99.4	6.5×10^{16}
11.2	n	10.4	4.3×10^{16}

Table 2: Electrical properties of Na-doped ZnO films by different processes.

Material	Mobility ($cm^2\ v^{-1}\ s^{-1}$)	Carrier concentration (cm^{-3})	References
ZnO:Na	1.41	5.19×10^{16}	[9]
ZnO:Na	0.138–0.676	6.90×10^{16}–2.16×10^{17}	[21]
ZnO:Na	0.22	5.3×10^{16}	[22]
ZnO:Na	0.43	2.5×10^{17}	[23]
ZnO:Na	0.402	1.81×10^{15}	[24]
ZnO:Na nanowires	2.1	1.3×10^{16}	[7]
ZnO:Na nanorod arrays	41.9–106	3.1×10^{16}–1.7×10^{17}	Our work

Figure 2 shows the surface morphologies of samples grown by simple aqueous solution approach on Si substrates. The nanorods are vertically well-aligned on the substrate surface. The diameter and length of pure ZnO are in the range of around 30 nm and 754 nm, respectively. Figure 3 shows a plot of diameter and length of ZnO nanorod arrays as functions of n_{Na}/n_{Zn}. With the increase of n_{Na}/n_{Zn}, the diameter of ZnO nanorod increased to 50 nm, 60 nm, 70 nm, and 70 nm, and the length decreased to 150 nm, 112 nm, 98 nm, and 71 nm, respectively.

Table 1 summarizes the electrical properties of ZnO films. Under Hall effect measurements, the undoped sample showed n-type conductivity, while the doped sample with n_{Na}/n_{Zn} of 2.8–8.4 showed p-type conductivity, but when n_{Na}/n_{Zn} was increased to 11.2, the film showed n-type conductivity again. In contrast, the electrical properties of samples with n_{Na}/n_{Zn} of 2.8–8.4 showed higher mobility and carrier concentration. Mobility was up to 106 $cm^2\ v^{-1}\ s^{-1}$ when n_{Na}/n_{Zn} was 2.8, and the carrier concentration was 1.7×10^{17} cm^{-3} when n_{Na}/n_{Zn} was 5.6. Mobility and carrier concentration were significantly improved by doping. We think this is due to the right amount of Na ions in the Zn lattice sites acting as acceptors, compensation Zn_i, and V_O intrinsic donor defects in the lattice. Most of the Na^+ occupies the lattice position, and the lattice expansion is small. The above XRD analysis further illustrates the rationality of our analysis. Electrical properties of Na-doped ZnO films by different processes are shown in Table 2. It can be seen that

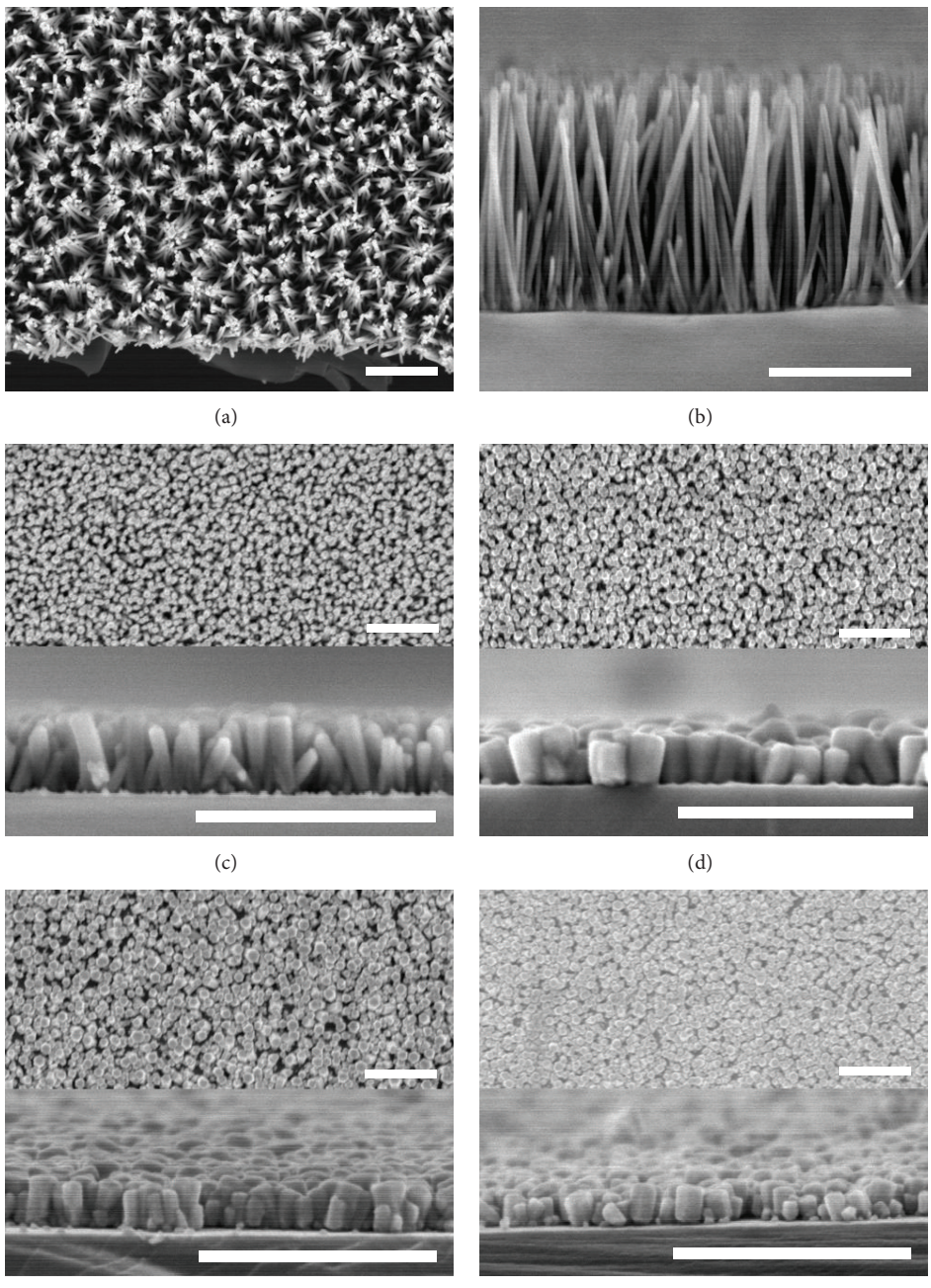

Figure 2: SEM images of the samples with n_{Na}/n_{Zn} of (a, b) 0, (c) 2.8, (d) 5.6, (e) 8.4, and (f) 11.2. All the scale bars are 500 nm.

Na-doped nanorod arrays in this study showed excellent electrical properties.

Usually, PL spectra of ZnO at room temperature were composed of a near band edge UV emission peak at around 375 nm and a deep level green emission peak at 450–550 nm. Researchers generally believe that the near band edge UV emission peak was caused by the recombination luminescence of the band edge exciton, while the deep level green emission peak was caused by the recombination of the defects such as O vacancy and Zn interstitial. Strong excitonic emission at 375 nm was observed, as shown in Figure 4. The UV emission was so strong, which indicates that all the 1D ZnO arrays were of high UV emission efficiency and that the green emission could hardly be observed in the PL spectrum, indicating that the crystalline quality of ZnO was high and lattice oxygen vacancy concentration is very low.

Figure 5 shows the doped samples before and after 325 nm excitation of Raman spectra. Raman spectra can be sensitive to detect the crystallization of the material and the defect state. Undoped Al (LO) mode peak at 578.1 cm^{-1} corresponds to the El longitudinal optical phonon (LO) mode. When the molar ratio of Na and Zn was 2.8, 5.6, 7.8, and 11.2, the peak position was at 577.3 cm^{-1}, 574.9 cm^{-1}, 574.2 cm^{-1}, and 575.8 cm^{-1}, which moved 0.8 cm^{-1}, 3.2 cm^{-1}, 3.9 cm^{-1},

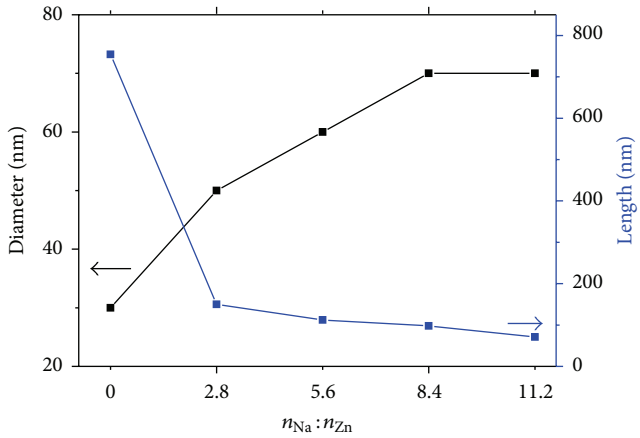

FIGURE 3: Diameter and length of ZnO nanorod arrays as functions of n_{Na}/n_{Zn}.

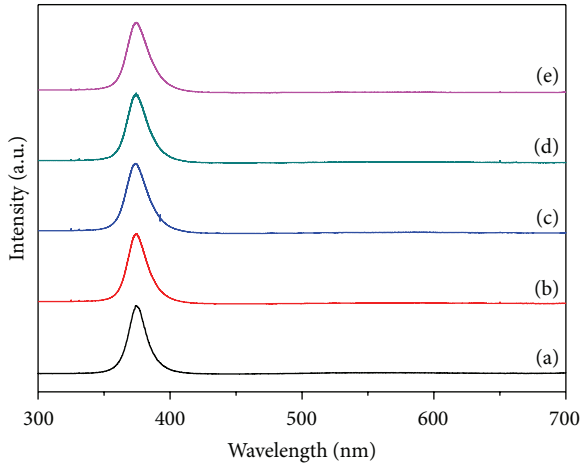

FIGURE 4: PL spectrum of the samples with n_{Na}/n_{Zn} of (a) 0, (b) 2.8, (c) 5.6, (d) 8.4, and (e) 11.2.

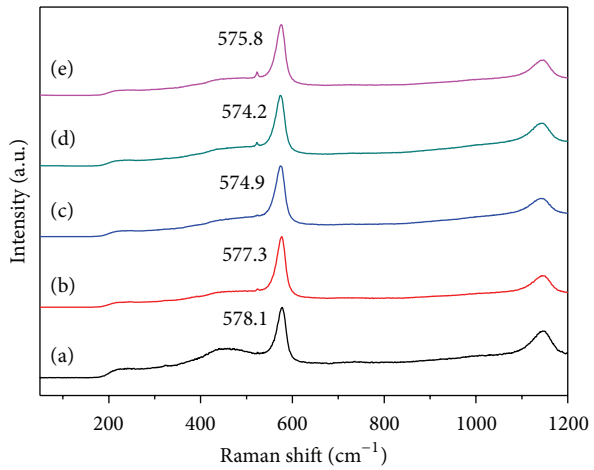

FIGURE 5: Raman spectra of the samples with n_{Na}/n_{Zn} of (a) 0, (b) 2.8, (c) 5.6, (d) 8.4, and (e) 11.2.

and 2.3 cm^{-1}, respectively. We observed that the peaks move to lower frequency, because this peak and the oxygen atom vacancies and zinc atoms interstitial related to its move reflect the changes in the concentration of free carriers in the ZnO crystal. So the concentration of free carriers in the ZnO crystals doped Na changed, and when the doping concentration of Al (LO) peak of the amount of movement is also different, this also shows the degree of change of free carrier concentration to be different.

4. Conclusion

In summary, Na-doped ZnO nanorod arrays with high crystalline quality were successfully fabricated on Si substrate by a simple hydrothermal method for the first time. With the increase of n_{Na}/n_{Zn}, the diameter of ZnO nanorod gradually increased from 30 nm to 70 nm, and the length decreased from 754 nm to 71 nm. Structural, electrical, and optical properties were investigated. The p-type carrier concentrations and mobility of Na-doped ZnO nanorod arrays arranged from 3.1×10^{16} cm^{-3} to 1.7×10^{17} cm^{-3} and 41.9 cm^2 v^{-1} s^{-1} to 106 cm^2 v^{-1} s^{-1}, respectively.

Competing Interests

The authors declare that there are no competing interests regarding the publication of this paper.

Acknowledgments

This study is supported by the National Natural Science Foundation of China (no. 51402252) and the Natural Science Foundation of Jiangsu Province (no. BK20140463).

References

[1] Y. X. Liu, H. L. Zhang, Z. X. Zhang, Y. Z. Xie, and E. Q. Xie, "Conversion of p-type to n-type conductivity in undoped ZnO films by increasing operating temperature," *Applied Surface Science*, vol. 257, no. 4, pp. 1236–1238, 2010.

[2] M. Ding, D. X. Zhao, B. Yao, B. H. Li, Z. Zhang, and D. Shen, "The p-type ZnO film realized by a hydrothermal treatment method," *Applied Physics Letters*, vol. 98, no. 6, Article ID 062102, 2011.

[3] Y. T. Shih, J. F. Chien, M. J. Chen, J. R. Yang, and M. Shiojiri, "P-type ZnO:P films fabricated by atomic layer deposition and thermal processing," *Journal of the Electrochemical Society*, vol. 158, no. 5, pp. H516–H520, 2011.

[4] V. Vaithianathan, B.-T. Lee, and S. S. Kim, "Preparation of As-doped *p*-type ZnO films using a Zn_3 As_2 ZnO target with pulsed laser deposition," *Applied Physics Letters*, vol. 86, no. 6, Article ID 062101, 2005.

[5] F. Friedrich, I. Sieber, C. Klimm, M. Klaus, C. Genzel, and N. H. Nickel, "Sb-doping of ZnO: phase segregation and its impact on p-type doping," *Applied Physics Letters*, vol. 98, no. 13, Article ID 131902, 2011.

[6] Y. J. Zeng, Z. Z. Ye, W. Z. Xu et al., "Dopant source choice for formation of p-type ZnO: Li acceptor," *Applied Physics Letters*, vol. 88, no. 6, Article ID 062107, 2006.

[7] W. Liu, F. X. Xiu, K. H. Sun et al., "Na-doped p-type ZnO microwires," *Journal of the American Chemical Society*, vol. 132, no. 8, pp. 2498–2499, 2010.

[8] L. Q. Zhang, Y. Z. Zhang, Z. Z. Ye et al., "The fabrication of Na doped p-type $Zn_{1-x}Mg_xO$ films by pulsed laser deposition," *Applied Physics A: Materials Science and Processing*, vol. 106, no. 1, pp. 191–196, 2012.

[9] Y. Li, Y. Z. Zhang, H. P. He, Z. Z. Ye, J. Jiang, and L. Cao, "Growth of Na doped p-type non-polar a-plane ZnO films by pulsed laser deposition," *Materials Letters*, vol. 76, pp. 81–83, 2012.

[10] M. K. Gupta, N. Sinha, and B. Kumar, "p-type K-doped ZnO nanorods for optoelectronic applications," *Journal of Applied Physics*, vol. 109, no. 8, Article ID 083532, 2011.

[11] M. A. Myers, J. H. Lee, Z. X. Bi, and H. Y. Wang, "High quality p-type Ag-doped ZnO thin films achieved under elevated growth temperatures," *Journal of Physics-Condensed Matter*, vol. 24, no. 22, Article ID 229501, 2012.

[12] B. Marí, M. Sahal, M. A. Mollar, F. M. Cerqueira, and A. P. Samantilleke, "p-Type behaviour of electrodeposited ZnO:Cu films," *Journal of Solid State Electrochemistry*, vol. 16, no. 6, pp. 2261–2265, 2012.

[13] C. H. Park, S. B. Zhang, and S.-H. Wei, "Origin of p-type doping difficulty in ZnO: the impurity perspective," *Physical Review B—Condensed Matter and Materials Physics*, vol. 66, no. 7, Article ID 073202, 2002.

[14] B. Y. Zhang, B. Yao, Y. F. Li et al., "Investigation on the formation mechanism of p-type Li-N dual-doped ZnO," *Applied Physics Letters*, vol. 97, no. 22, Article ID 222101, 2010.

[15] M. Suja, S. B. Bashar, M. M. Morshed, and J. L. Liu, "Realization of Cu-doped p-type ZnO thin films by molecular beam epitaxy," *ACS Applied Materials & Interfaces*, vol. 7, no. 16, pp. 8894–8899, 2015.

[16] S. B. Bashar, M. Suja, M. Morshed, F. Gao, and J. Liu, "An Sb-doped p-type ZnO nanowire based random laser diode," *Nanotechnology*, vol. 27, no. 6, Article ID 065204, 2016.

[17] L. Cao, L. P. Zhu, J. Jiang, Y. Li, Y. Z. Zhang, and Z. Z. Ye, "Preparation and properties of p-type Ag-doped ZnMgO thin films by pulsed laser deposition," *Journal of Alloys and Compounds*, vol. 516, pp. 157–160, 2012.

[18] X. Fang, J. H. Li, D. Zhao, D. Shen, B. Li, and X. Wang, "Phosphorus-doped p-Type ZnO nanorods and ZnO nanorod p-n homojunction LED fabricated by hydrothermal method," *Journal of Physical Chemistry C*, vol. 113, no. 50, pp. 21208–21212, 2009.

[19] S. N. Das, J.-H. Choi, J. P. Kar, T. I. Lee, and J.-M. Myoung, "Fabrication of p-type ZnO nanowires based heterojunction diode," *Materials Chemistry and Physics*, vol. 121, no. 3, pp. 472–476, 2010.

[20] Q. X. Xia, K. S. Hui, K. N. Hui et al., "High quality p-type N-doped AZO nanorod arrays by an ammonia-assisted hydrothermal method," *Materials Letters*, vol. 78, pp. 180–183, 2012.

[21] Z. Zheng, Y. F. Lu, Z. Z. Ye, H. P. He, and B. H. Zhao, "Carrier type- and concentration-dependent absorption and photoluminescence of ZnO films doped with different Na contents," *Materials Science in Semiconductor Processing*, vol. 16, no. 3, pp. 647–651, 2013.

[22] X. H. Pan, Y. S. Zhou, S. S. Chen et al., "Effect of Na contents on fabrication of p-type non-polar m-plane ZnO films," *Journal of Crystal Growth*, vol. 404, pp. 54–58, 2014.

[23] W. Chen, X. H. Pan, S. S. Chen et al., "Investigation on non-polar m-plane ZnO and Na-doped p-type ZnO films grown by plasma-assisted molecular beam epitaxy," *Applied Physics A: Materials Science and Processing*, vol. 121, no. 1, pp. 77–82, 2015.

[24] P. Ding, X. H. Pan, Z. Z. Ye et al., "Realization of p-type non-polar a-plane ZnO films via doping of Na acceptor," *Solid State Communications*, vol. 156, pp. 8–11, 2013.